

IEICE Proceeding Series

“Realistic” Electronic Neuron

Elena Tamaševiciute, Gytis Mykolaitis, Arunas Tamaševicius

Vol. 1 pp. 860-863

Publication Date: 2014/03/17

Online ISSN: 2188-5079

Downloaded from www.proceeding.ieice.org

“Realistic” Electronic Neuron

Elena Tamaševičiūtė¹, Gytis Mykolaitis^{1,2} and Arūnas Tamaševičius¹

¹Laboratory of Nonlinear Electronics, Department of Electronics, Center for Physical Sciences and Technology
 11 A. Goštauto, Vilnius, LT-01108 Lithuania

Email: elena.tamaseviciute@yahoo.com, tamasev@pfi.lt

²Department of Physics, Faculty of Fundamental Sciences, Vilnius Gediminas Technical University
 11 Saulėtekio, Vilnius, LT-10223 Lithuania

Email: gyttis@pfi.lt

Abstract– An electronic circuit, imitating spiking trains from real neurons, is described. The electronic neuron is a Wien-bridge based circuit with a super-linear spike mechanism. Numerical simulations using ELECTRONICS WORKBENCH and MATHEMATICA software, also hardware experiments have been performed. The characteristics of the spikes are the following: spike height is 100 mV, spike width is 1 ms, and interspike interval is 100 ms.

1. Introduction

Besides analytical and numerical studies of the different neuron models, efforts have been concentrated on designing and building electronic neurons. Replacement of biological neurons with electronic devices, governed by simple equations, can contribute to a better understanding of the biological effects. A large number of nonlinear electrical circuits imitating behavior of neurons have been described in the literature [1-9]. Among them are various modifications of the FitzHugh–Nagumo (FHN) electronic neurons [1-5], class-I excitable system exhibiting Andronov bifurcation [6], the Hodgkin–Huxley type [7], and the Liao's time delayed [8] electronic cells. Recently a network of 30 FHN coupled electronic neurons has been described [9]. In the most cases electronic neurons have been treated as formal imitators and no care has been taken about the scale of the output signals. For example, the amplitude of the pulses (spikes) generated by the electrical circuits is of several volts, the pulse interval in the spike trains ranges from several tens of microseconds to several tens of milliseconds. Indeed, this is not important when the electronic circuits are used to imitate dynamical behavior of neurons only. However, when designing and building various electronic controllers of the neuronal systems, e.g. deep brain stimulators, it is necessary to adjust them to the real scales. Therefore it makes sense to design electronic neurons, operating on the real scales, both in time and in amplitude domains. In this paper, we suggest an electronic circuit, generating spike trains with parameters close to those generated in the real neurons. Typical spike parameters observed in neurons are the following: spike height is about 100 mV, spike width is about 1 ms, interspike intervals ranges from several hundreds to several tens of milliseconds [10].

2. Circuit

The oscillator is the Wien-bridge (R1C1–R2C2) based circuit (Fig. 1). The OA is the NE5534 type operational amplifier, a linear and non-inertial active device; the nonlinear devices D1, D2, and D3 are the SB160 type Schottky diodes with reverse current $2 \cdot 10^{-7}$ A (at -0.5 V).

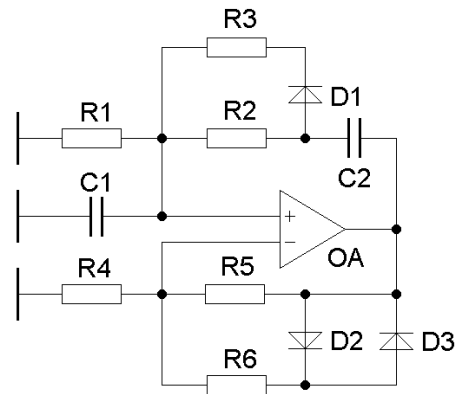


Fig. 1. Circuit diagram of electronic neuron.

3. Equations

Dynamics of the circuit in Fig.1 is described by the following set of equations:

$$\begin{aligned} C_1 \frac{dV_1}{dt} &= \frac{V_0 - V_1 - V_2}{R_2} + I_{D1} f(V_{D1R3}) - \frac{V_1}{R_1}, \\ C_2 \frac{dV_2}{dt} &= \frac{V_0 - V_1 - V_2}{R_2} + I_{D1} f(V_{D1R3}), \end{aligned} \quad (1)$$

where V_1 and V_2 is the voltage across the capacitor C1 and C2, respectively. The $V_0(V_1)$ is the nonlinear output voltage of the operational amplifier OA (nonlinearity of the output is introduced by the diodes D2 and D3 inserted in the negative feedback loop). The I_{D1} is the nonlinear current through the diode D1, V_{D1R3} is the voltage across the series composite D1–R3.

We use a piecewise linear approximation of the nonlinear characteristics $I_{DR}=f(V_{DR})$ of the all D–R composites, namely D1–R3, D2–R6, and D3–R6:

$$I_{DR} = \begin{cases} 0, & V_{DR} \leq V^* \\ \frac{V_{DR} - V^*}{R + r_d}, & V_{DR} > V^* \end{cases} \quad (2)$$

Here V^* is the breakpoint voltage and r_d is the differential resistance of a diode.

After introducing the following dimensionless variables and parameters

$$\begin{aligned} x &= \frac{V_1}{V^*}, \quad y = \frac{V_2}{V^*}, \quad g = \frac{t}{R_1 C_1}, \\ a &= \frac{R_1}{R_2}, \quad b = \frac{R_1}{R_3 + r_d}, \\ k_1 &= \frac{R_5}{R_4} + 1, \quad k_2 = \frac{R_6 + r_d}{R_4} + 1, \end{aligned} \quad (3)$$

also assuming for simplicity $C_1=C_2$, a set of dimensionless differential equations for the circuit in Fig. 1, convenient for numerical simulation can be derived:

$$\begin{aligned} \dot{x} &= aF_1(x, y) + bF_2(x, y) - x, \\ \dot{y} &= aF_1(x, y) + bF_2(x, y), \end{aligned} \quad (4)$$

where the nonlinear functions are:

$$\begin{aligned} F_1(x, y) &= g(x) - x - y, \\ F_2(x, y) &= [g(x) - x - y - 1]H[g(x) - x - y - 1], \\ g(x) &= \begin{cases} \frac{k_1(k_2x - 1)}{k_1 + k_2}, & x < -\frac{1}{k_1} \\ k_1x, & |x| \leq \frac{1}{k_1} \\ \frac{k_1(k_2x + 1)}{k_1 + k_2}, & x > \frac{1}{k_1} \end{cases}. \end{aligned} \quad (5)$$

In the limit of $k_1 \rightarrow \infty$ ($R_5 \gg R_4$) and assuming $k_1 \gg k_2$ ($R_6 \gg R_4$), the three-segment nonlinear output function $g(x)$ can be approximated by

$$g(x) = k_2x + \text{sgn } x. \quad (6)$$

Consequently the nonlinear functions $F_1(x, y)$ and $F_2(x, y)$ can be simplified to:

$$\begin{aligned} F_1(x, y) &= (k_2 - 1)x - y + \text{sgn } x, \\ F_2(x, y) &= [(k_2 - 1)x - y]H[(k_2 - 1)x - y]. \end{aligned} \quad (7)$$

In $F_2(x, y)$ we made use of the fact that the Heaviside function $H(x, y)$ in our case becomes nonzero at the positive values of x only. Therefore, in $F_2(x, y)$ we have $\text{sgn } x=1$ and $\text{sgn } x-1=0$. Finally, we come to a compact set of differential equations:

$$\begin{aligned} \dot{x} &= a(kx - y + \text{sgn } x) + b(kx - y)H(kx - y) - x, \\ \dot{y} &= a(kx - y + \text{sgn } x) + b(kx - y)H(kx - y). \end{aligned} \quad (8)$$

The notation $k=k_2-1$ is used here. The terms in (8), containing the $H(u)$, are essentially super-linear functions. They approximate the exponential spike mechanism [11].

3. Numerical Results

3.1. Circuit Simulation

Computer simulation of the circuit in Fig. 1 was performed using the ELECTRONICS WORKBENCH PROFESSIONAL (EWB) software. The following circuit element values were used: $R_1 = 1 \text{ k}\Omega$, $R_2 = 180 \text{ k}\Omega$, $R_3 = 360 \Omega$, $R_4 = 100 \Omega$ (adjustable), $R_5 = 20 \text{ k}\Omega$, $R_6 = 100 \Omega$, $C_1 = C_2 = 470 \text{ nF}$. Simulation with $R_4 = 80 \Omega$ is illustrated in Fig. 2. The interspike interval $T_0 \approx 100 \text{ ms}$.

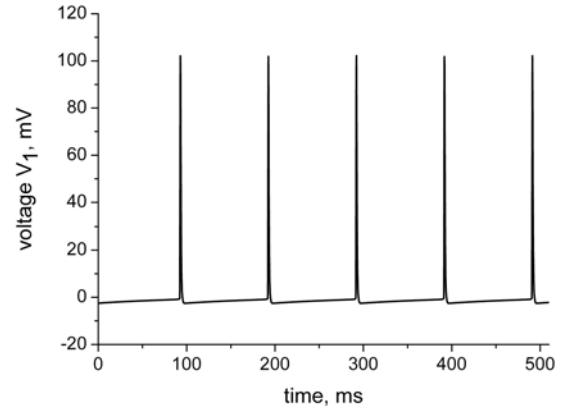


Fig. 2. Voltage $V_1(t)$ across capacitor C1 simulated by means of the EWB.

3.2. Equation Simulation

Eq.(7) were integrated by means of the MATHEMATICA package. The following parameters were used: $V^* = 0.17 \text{ V}$, $R_1 C_1 = 0.5 \text{ ms}$, $R_4 = 72 \Omega$, $r_d = 80 \Omega$ (r_d depends on current through the diode; here it was evaluated at an average current of $\approx 0.3 \text{ mA}$), $a = 0.005$, $b = 2.3$, $k_1 = 250$, and $k_2 = 3.5$. Result is plotted in Fig. 3. One can see, that the $T_0 \approx 90 \text{ ms}$, that is by 10% shorter than in the EWB simulation. This can be explained by the fact, that in (5) we use a simplified, piecewise-linear function for the current through the diode-resistor composites. It includes two somewhat freely adjustable parameters, the voltage V^* and the resistance r_d . The latter strongly influences the parameters b and k_2 and eventually the interval T_0 .

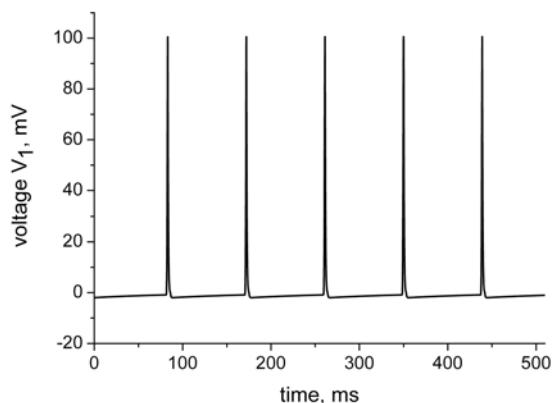


Fig. 3. Voltage $V_1(t)$ across capacitor C1 from (3).

4. Experimental Results

A snapshot of the spike train generated by the circuit with $R_4 = 72 \Omega$ and taken from the screen of an analogue oscilloscope is presented in Fig. 4. Spike amplitude is $A \approx 100$ mV, interspike interval $T_0 \approx 100$ ms (Fig. 4a). The spike width T_1 has been measured using faster sweep (0.5 ms/div.) of the oscilloscope. Half-amplitude pulse duration $T_1 \approx 1$ ms. The interval T_0 can be tuned by means of the resistor R_2 . For example, the interval can be reduced from $T_0 \approx 100$ ms at $R_2 = 180$ k Ω to $T_0 \approx 50$ ms at $R_2 = 90$ k Ω (Fig. 4b). We note, that R_4 should be slightly increased to keep the same amplitude of 100 mV.

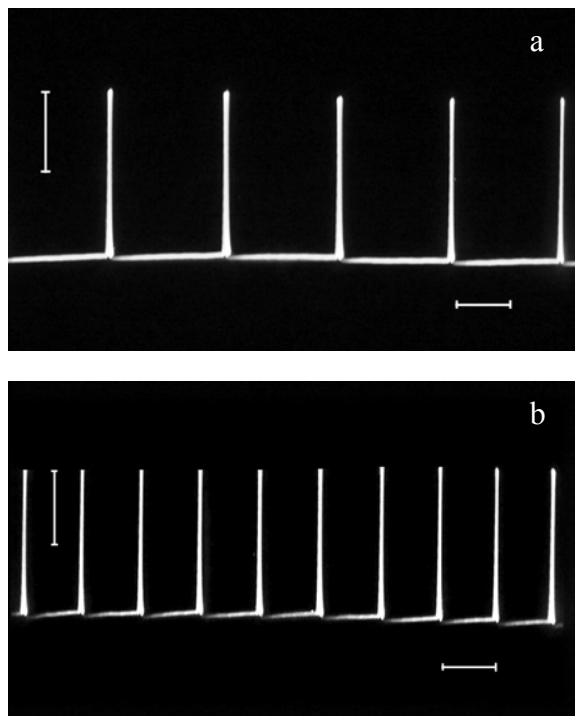


Fig. 4. Voltage $V_1(t)$ across capacitor C1 from hardware circuit. Scales: vertical 50 mV, horizontal 50 ms. (a) $R_2 = 180$ k Ω , (b) $R_2 = 90$ k Ω .

The electronic neuron has been tested for the possibility to control its steady state [4, 5]. An auxiliary RC first order filter ($R \leq 510 \Omega$, $C \geq 100 \mu\text{F}$), when connected to the capacitor C1, was able to suppress the spike trains and to stabilize an *a priori* unknown unstable non-zero steady state $V_{10} \approx -0.5$ mV. The non-zero value of the steady state in the electronic neuron appeared because of the unavoidable input offsets of the nonideal OA.

In addition, “high frequency” periodic signals, known as the ‘deep brain stimulation’ (DBS) [12-14], e.g. in the Parkinson’s disease therapy, when applied to the capacitor C1, suppress the spikes (Fig. 5).

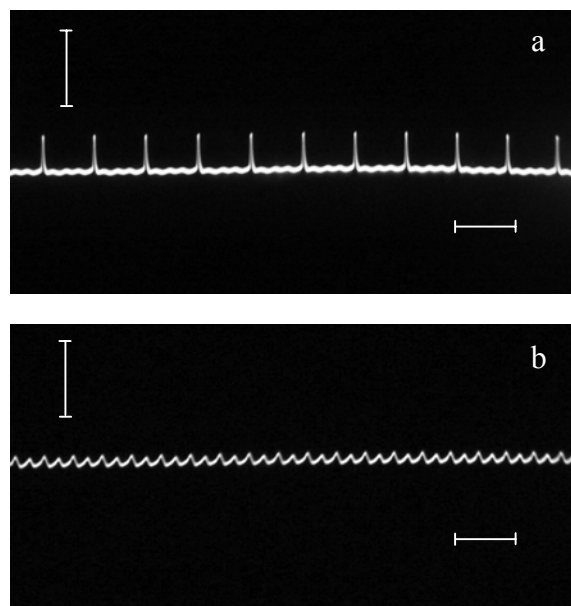


Fig. 5. Voltage $V_1(t)$ across capacitor C1 from hardware circuit with the “DBS”: $I_p \sin(2\pi ft)$; $f = 100$ Hz. At $I_p = 0$ $V_{1\text{max}} = 100$ mV, $T_0 = 100$ ms (see Fig. 4a). Scales: vertical 50 mV, horizontal 50 ms. (a) $I_p = 0.5 \mu\text{A}$, (b) $I_p = 1.0 \mu\text{A}$.

The threshold value of the I_p , sufficient to suppress the spikes, depends on the frequency of perturbation (Fig. 6).

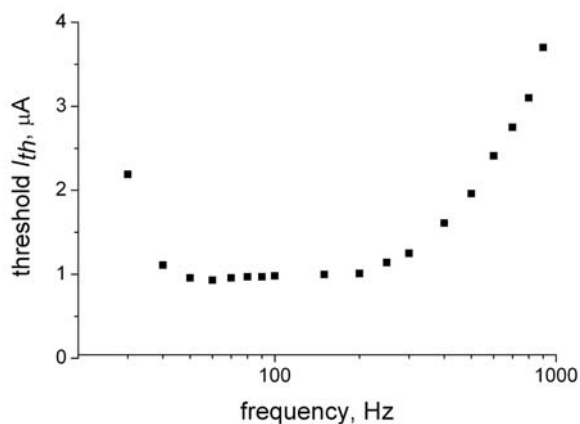


Fig. 6. Threshold perturbation current I_{th} versus frequency.

The frequency dependence of threshold perturbation current is surprisingly similar to that observed in the therapeutic DBS, with the best suppression between 50 and 200 Hz. We have set perturbation frequency to 100 Hz, exactly the same as in the Benabid's experiment [12]. In addition, the sine waveform perturbation was replaced with periodic rectangular pulses, yielding the same effect of spike suppression.

5. Comparison with the Ingrate-and-Fire Circuit

We note, that the one-dimensional Integrate-and-Fire (I&F) circuit (Fig. 7) under appropriate selection of the circuit parameters can exhibit similar spike trains (Fig. 8).

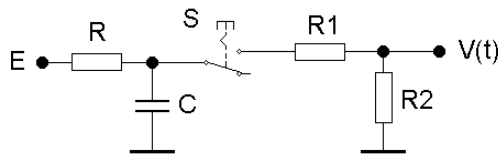


Fig. 7. Circuit diagram of an I&F electronic neuron. S is a switch, controlled by voltage $V_c(t)$.

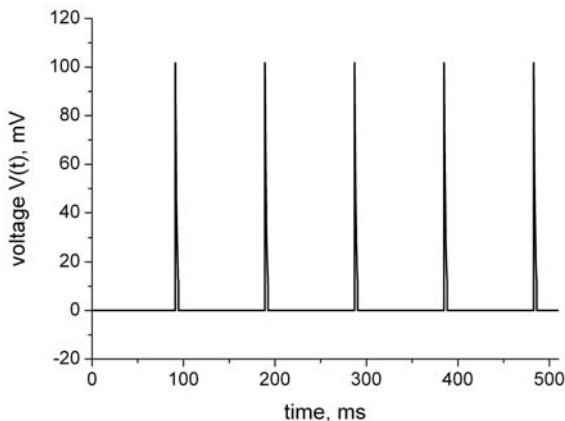


Fig. 8. Output voltage $V(t)$ in Fig. 7, simulated by means of the EWB. $E = 10$ V, $R = 10$ k Ω , $C = 100$ μ F, $R_1 = 12$ Ω , $R_2 = 1.5$ Ω . Control parameters of the switch: turn-on voltage 1 V, turn-off voltage 0.1 V.

However, the 'I&F' one-dimensional electronic neuron allows neither stabilization of the steady state by means a simple first order RC filter (as described in Section 4) nor spike suppression by means of the "DBS".

6. Conclusions

We have designed, build and investigated an electronic imitator of a spiking neuron. The parameters of the spike trains are close to those observed in real neurons [10], i.e. the spike height of about 100 mV, spike width is about 1 ms, and interspike interval is about 100 ms (tunable). The "realistic" two-dimensional electronic imitator admits its control by means of a tracking RC filter [4,5] and the "deep brain stimulation" technique [12-14].

References

- [1] S. Binczak, V. B. Kazantsev, V. I. Nekorkin, and J. M. Bilbaut, "Experimental study of bifurcations in modified FitzHugh–Nagumo cell," *Electron. Lett.*, vol.39, pp.961–962, 2003.
- [2] S. Jacquir, S. Binczak, J. M. Bilbaut, V. B. Kazantsev, and V. I. Nekorkin, "Study of electronic master-slave MFHN neurons," *Proc. 12th International Workshop on Nonlinear Dynamics of Electronic Systems, NDES'2004*, 2004, Évora, Portugal, pp.182-185. Centro de Geofisica de Évora, Universidade de Évora, 2004.
- [3] S. Jacquir, S. Binczak, J. M. Bilbaut, V. B. Kazantsev, and V. I. Nekorkin, "Synaptic coupling between two electronic neurons," *Nonlin. Dyn.*, vol.44, pp.29–36, 2006.
- [4] E. Tamaševičiūtė, A. Tamaševičius, G. Mykolaitis, S. Bumelienė, R. Kirvaitis, and R. Stoop, "Electronic analog of the FitzHugh-Nagumo neuron model and noninvasive control of its steady state," *Proc. 17th International Workshop on Nonlinear Dynamics of Electronic Systems, NDES'2009*, 21-24 June, 2009, Rapperswil, Switzerland, p.138-141, USB Memflash.
- [5] A. Tamaševičius, E. Tamaševičiūtė, G. Mykolaitis, S. Bumelienė, R. Kirvaitis, and R. Stoop, "Neural spike suppression by adaptive control of an unknown steady state," *Lecture Notes Comp. Sci.*, vol.5768, pp.618–627, 2009.
- [6] J. Aliaga, N. Busca, V. Minceș, G. B. Mindlin, B. Pando, A. Salles, and L. Sczupak, "Electronic neuron within a ganglion of a leech (*Hirudo Medicinalis*)," *Phys. Rev. E*, 2003, **67**, (6), 061915
- [7] J. D. Sitt and J. Aliaga, "Versatile biologically inspired electronic neuron," *Phys. Rev. E*, vol.76, 051919, 2007.
- [8] S. Duan and X. Liao, "An electronic implementation for Liao's chaotic delayed neuron model with nonmonotonous activation function," *Phys. Lett. A*, vol.369, pp.37-43, 2007.
- [9] E. Tamaševičiūtė, G. Mykolaitis, and A. Tamaševičius, "Analogue modelling an array of the FitzHugh-Nagumo oscillators," *Nonlinear Analysis: Modelling and Control*, vol.17, pp.118-125, 2012.
- [10] W. Gerstner and W. Kistler, *Spiking neuron models*, Cambridge University Press, Cambridge, 2005.
- [11] R. Brette and W. Gerstner, "Adaptive exponential integrate-and-fire model as an effective description of neuronal activity," *J. Neurophys.*, vol.94, pp.3637-3642, 2005.
- [12] A. L. Benabid, P. Pollak, A. Louveau, S. Henry, and J. Derougemont, "Combined (thalamotomy and stimulation) stereotactic surgery of the vim thalamic nucleus for bilateral Parkinson disease," *Appl. Neurophys.*, vol.50, pp.344-346, 1987.
- [13] A. L. Benabid, A. Benazzous, and P. Pollak, "Mechanisms of deep brain stimulation," *Mov. Disorders*, vol.17, (suppl.3), pp. S73-S74, 2002.
- [14] E. B. Montgomery and J. T. Gale, "Mechanisms of deep brain stimulation (DBS)," *Neurosci. Biobehavioral Rev.*, vol.32, pp.388-407, 2008.